Monte Carlo Simulations of End-Adsorption of Head-to-Tail Reversibly Associated Polymers

Chun-Chung Chen and Elena E. Dormidontova*

Department of Macromolecular Science and Engineering, Case Western Reserve University, Cleveland, Ohio 44106

Received June 2, 2006; Revised Manuscript Received August 25, 2006

ABSTRACT: Using Monte Carlo simulations we study reversible end-adsorption of head-to-tail associating polymers on a surface containing adsorption sites. The adsorption energy was considered to be similar to the association energy ($10kT$) leading to the competition between association in the bulk and adsorption. We found that for all considered volume fractions of polymer in the bulk Φ and all densities of adsorption sites σ the density profile of adsorbed polymer layer follows an exponential dependence ($\sim\exp(-r/\xi)$, with the decay length ξ being a function of the average chain length in the bulk and independent of σ). The chain length distribution for adsorbed polymer follows a similar exponential dependence as in the bulk, except for an enhancement of short chains in the distribution, especially for large σ. With an increase in σ adsorbed polymers start to overlap leading to a decrease in the chain length to avoid stretching. Up to a certain concentration σ_{cr} the fraction of occupied sites on the surface remain nearly constant. At $\sigma \geq \sigma_{cr}$ adsorbed oligomers start to overlap leading to a decrease in the fraction of occupied sites. Because of the reversibility of association adsorbed chains are not stretched in the adsorbed layer, as the average radius of gyration of the chains remains equal to that for bulk polymers. At a low density of adsorption sites, the height of the adsorbed polymer layer is defined by the average radius of gyration for adsorbed chains, as expected for the mushroom regime. With an increase in σ, the average height of the polymer layer adsorbed from concentrated solutions increases, while for polymer layers adsorbed from more dilute solutions the height remains practically at the same level or even slightly decreases. The increase of the height for larger Φ is due to the chain orientation along the surface normal. At low σ chains adsorbed from relatively concentrated solutions are preferably oriented along the surface (due to the narrow depletion zone). With an increase in σ, chains become more crowded at the surface and start to orient away from it leading to an increase in the height of the adsorbed layer. Different regimes of the adsorbed chain behavior are summarized in the diagram of states, which can be applied for systems with different adsorption energies or spacer lengths.

1. Introduction

In recent decades, supramolecular polymers have attracted growing attention in scientific research. Successful synthetic efforts have made available a variety of reversible complexes based on multiple hydrogen bonding, complementary DNA sequences, or metal−ligand coordination bonds.[1−3] Possessing a considerable strength of association, while retaining the advantages of reversible bonding, this new class of materials combines the properties of traditional synthetic polymers with the versatility of biomolecules. The reversibility of association allows one to control the degree of polymerization, chain architecture and physical properties of these polymers depending on external conditions (temperature, force fields, solvent composition, pH, etc.) which may find application in the general area of "smart materials".

The self-healing nature of these polymers, which makes their properties so unique, also provides considerable challenges to the experimental characterization of these materials. Only in recent years have experimental reports on the physical properties of these polymers become more common. One of the recent interesting developments in this area is the application of atomic force microscopy (AFM) techniques to study the behavior of these polymers end-grafted to surfaces. Besides studying the strength of association of individual complexes,[4−6] AFM measurements could also provide insight on the chain length distribution and thickness of the end-grafted/end-adsorbed layer as well as its adhesive properties as a function of grafting density and strength of association.[7−9]

* Corresponding author. E-mail: eed@case.edu.

Theoretical (analytical and simulation) studies of reversibly associated polymers have certain advantages over the experimental approaches as the former allows us to explore the microscopic details of polymer behavior under various conditions without the complications of characterization and synthetic challenges experienced by the latter. As a result it is not surprising that theoretical studies devoted to reversibly associated polymers exceed in number the experimental ones. Theoretical models go back to the classical Flory−Stockmayer approach for condensation polymerization,[10,11] further expanded by Cates and co-workers for the case of "living polymers",[12] and followed by many other detailed models on supramolecular assembly in the bulk.[13−15] The behavior of supramolecular polymers near surfaces was also studied by several theoretical groups providing predictions for the chain length distribution in a gap,[16−20] chain orientation near the surface,[16] depletion width at a neutral surface,[19,21] and adsorption on attractive surfaces.[21]

Much less theoretical attention so far was attracted to the behavior of end-adsorbed supramolecular polymers. We are aware of only three theoretical papers in this area.[22−24] Milchev and co-workers have studied "living polymerization" from a surface using canonical off-lattice Monte Carlo simulations.[22] van der Gucht and Besseling et al.[23] have used a lattice-based self-consistent field model to calculate the interaction between two surfaces induced by end-adsorbing supramolecular polymers of different types. In the more recent paper they apply a mean-field Gaussian chain approximation to predict the density distribution, surface excess and average chain length of end-adsorbed polymers in the limit of high dilution and small

10.1021/ma061236b CCC: $33.50
Published on Web 11/20/2006

adsorption densities.[24] In all cases,[22−24] the size of a repeat unit was equal to one monomer, whereas experimentally a repeat unit of supramolecular polymers consists of at least two associating units separated by a finite length spacer (often of a different flexibility).[1−3] So far no predictions have been made regarding the height of adsorbed polymers, which is probably the most reliable information that can be gained from experimental studies. Additionally the effect of the density of adsorption sites on the properties of the adsorbed layer was totally unexplored. Our current paper has the aim to fill this gap in the theoretical understanding of the behavior of head-to-tail associated polymers and provide predictions for the chain length distribution, fraction of occupied adsorption sites and height of the adsorbed polymer layer as functions of volume fraction of polymer in the bulk and density of adsorption sites. We expect that our results will provide guidance for ongoing experimental studies and attract further attention by the theoretical community.

End-adsorption of supramolecular polymers from the bulk is expected to have some common features with end-adsorption of chemically bonded polymers. The latter was studied extensively both theoretically[25−32] and experimentally[33−36] especially for the case of diblock copolymer adsorption. For the case of a very short adsorbing block or end-adsorbing chemically bonded polymers, it was found that a larger degree of surface coverage is achieved for polymers of low molecular weight with a higher energy of adsorption when adsorbed from concentrated solutions.[25,26,28,30] The adsorbed chains are not expected to be fully stretched unless the adsorption energy is very high.[25,26,28,31] The overall height of adsorbed layer is expected to increase with an increase of adsorption energy, polymer concentration in the bulk and chain length.[26,31] On the basis of what is known for chemically bonded monodisperse polymers, an increase in concentration is expected to increase the surface coverage, but on the other hand, adsorption of longer chains should produce lower surface coverage. Thus, for reversibly associated polymers which form longer chains at larger bulk polymer concentration these two effects should counteract each other. Additionally the chain length of adsorbed polymers can be different from that in the bulk making the overall results of adsorption even more complicated. Having in mind these important differences between the reversibly associated and chemically bonded polymers, using the Monte Carlo simulation technique we intend to address in this paper the following questions: (i) will the monomer density profile for adsorbed polymers follow an exponential dependence only for low concentration and low surface coverage (as predicted in ref 24) or it will be more like the power law dependence observed for living polymerization from the surface?[22,37] (ii) What will be the chain length distribution for adsorbed polymers and how it will change with the density of adsorption sites and bulk polymer concentration? (iii) Will surface coverage increase or decrease with an increase of polymer bulk concentration (and hence increase of average chain length in the bulk)? (iv) Will the polymer chains be stretched in the adsorbed polymer layers (i.e., can the brush regime be achieved)? (v) How will the height of adsorbed polymer layer change with an increase in polymer concentration in the bulk and density of adsorption sites?

This paper will be organized as follows. In the next section, we will present the details of our simulation approach. Then we will discuss the obtained results concerning the density profiles, chain length distribution of adsorbed polymers, surface coverage and height of adsorbed polymer layer. The following section on "diagram of states for end-adsorbed head-to-tail reversibly associated polymers" will summarize different regimes of behavior of adsorbed polymers. We will close the paper with conclusions on the main findings of this study.

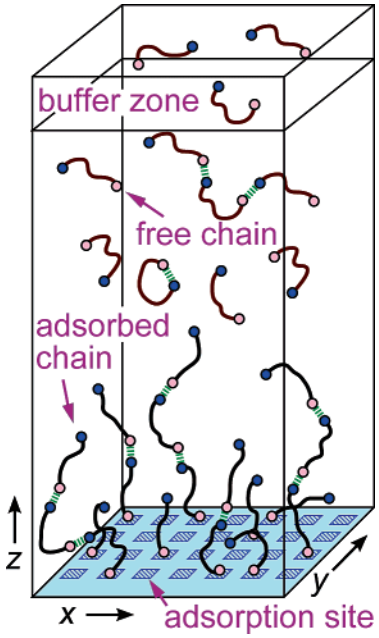

Figure 1. Schematic presentation of reversible end-adsorption of head-to-tail associating polymers in a simulation box. Periodic boundary conditions are enforced in x and y directions. A constant chemical potential is ensured by inserting/removing oligomers to/from the buffer zone.

2. Simulation Details

To study end-adsorption of reversibly associated polymers, we employ Monte Carlo (MC) simulations using the bond-fluctuation model (BFM).[38] The reversibly associated polymers consist of oligomers containing $N_o = 4$ (unless specified differently) monomers each including one donor and one acceptor group at the ends. The size of a donor or an acceptor is assumed to be the same as the size of a regular monomer in this study. A free donor (not associated with an acceptor) is capable of forming a reversible (hydrogen) bond with a free acceptor. Each of such associations lowers the energy of the system by the association energy $\Delta E_{compl} = 10kT$ (unless specified differently). To account for the orientational specificity of a donor−acceptor association, we considered energy $E_{st}(\theta) = B(1 - \cos\theta)$ with $B = 5kT$ for any bond angle θ between adjacent segments involving a reversible bond.[15] All chemical bonds of an oligomer are assumed to be completely flexible ($B = 0$) in this study. To account for excluded volume in the BFM, the distance between the monomers (connected by chemical or reversible bonds) is limited to the following values: $l = 2a$, $\sqrt{5}a$, $\sqrt{6}a$, $3a$, or $\sqrt{10}a$, where a is the unit spacing of the cubic lattice.

The adsorbing surface was implemented by placing a wall with homogeneously distributed adsorption sites at $z = 0$. In the x- and y-directions we use periodic boundary conditions, so that our simulation box was $L_x = L_y = 64a$ and $L_z = 128a$. In our simulations we assumed that the adsorption occurs only by formation of a reversible bond between an adsorption site on the surface and a free donor group of an oligomer separated from it by the minimal possible distance ($2a$) in the z-direction (Figure 1).

We note that orientation of the oligomer plays no role in the success of the adsorption attempt as long as its donor is in the

correct position with respect to an adsorption site. The energy of the system is lowered for each adsorbed donor by ΔE_{ads} which was chosen to be the same as the association energy, i.e., $\Delta E_{ads} = \Delta E_{compl}$ ($= 10kT$, unless specified differently). Since acceptors or regular monomers of an oligomer could not adsorb on the surface, the formation of loops and trains is excluded. Taking into account the excluded volume of monomers, this implies that polymers can only move within the range of $2a \le z \le 126a$. This effectively creates a closed boundary condition in the z direction of the system. To maintain constant polymer bulk concentration for the different density of adsorption sites on the surface, we keep constant the chemical potential for oligomers (rather than constant number of oligomers). This has been achieved by considering equilibrium with the buffer zone located at the far end of the simulation box ($123a \le z \le 126a$). First, we model the reversibly associated polymers with no adsorption sites on the surface. For each bulk volume fraction Φ considered, we maintained a fixed integer number $\mathcal{D}$ of donors in the buffer zone. For the value of Φ, we took the plateau value of the monomer volume density profile between the walls $z = 0$, $z = 128$. Then adsorption sites were introduced and system was allowed to equilibrate while maintaining the same number of donors in the buffer zone $\mathcal{D}$ as in the absence of the adsorption sites. The number of donors in the buffer zone were checked every 128 Monte Carlo time steps and if it was larger than $\mathcal{D}$, an excess number of oligomers with their donors having the largest z coordinates were deleted from the system; if this number was less than $\mathcal{D}$, missing oligomers were inserted near the far end ($z = 126a$) of the system.

Following the standard BFM procedure, the MC update of the system is performed by randomly choosing one monomer and attempting its movement to a randomly chosen nearest neighbor site. The move is rejected if it violates the space constraints described above. Otherwise, as prescribed by the Metropolis algorithm,[39] the move is accepted with the probability $P = \min[1, e^{-\Delta E/(kT)}]$, where $\Delta E = \Delta E_{new} - \Delta E_{old}$ is the energy difference between the new and the old configuration of the system. This energy difference comes from the energetic gain for formation of a reversible bond between a donor and an adsorption site ΔE_{ads} and the entropic penalty of bending a reversible bond ΔE_{st}. If the selected monomer is not a donor, then the moving attempt is completed and next monomer is selected for an MC update. If it is a donor, then in addition to the moving attempt, we also perform a reversible bond update: if there are free acceptors in a bonding distance from the donor, a reversible bond is formed with an available free acceptor with the probability $Ce^{\Delta E_x/(kT)}$, (where ΔE_x is the energy change of the system for the formation of the bond) or no bonds will be formed with probability $C = (1 + \sum_{i=1}^{N_a} e^{\Delta E_i})^{-1}$ (where N_a is the total number of available free acceptors for this donor). If a donor was reversibly bonded prior to the move, this reversible bond will be broken and bonding update will be performed as described above. As a result of the bonding update a new reversible bond can be formed or old one restored or no bonds formed at all depending on the corresponding probabilities. We note that in order to obtain the probability of reversible bond formation all neighboring free acceptors have to be checked and the energy of each possible bond has to be calculated. A free acceptor for which formation of a reversible bond with the current donor would intersect with any existing bond was disregarded in these considerations. We note that this method of bonding update is different from the commonly used Metropolis algorithm but it also satisfies detailed balance. As the new bonding configuration of the system is directly drawn from the Boltzmann probability distribution, the system has a minimal potential barrier for the bonding-unbonding event in this case[12b] resulting in fast equilibration for the reversible bonding. A Monte Carlo time step (MCts) is defined as the number of MC updates equal to the number of monomers in the system. It corresponds to the simulation time during which each monomer has a chance to make one moving attempt on average. All systems were allowed to equilibrate for no less than $2^{22} \approx 4 \times 10^6$ MCts before measurements are made and averaged over subsequent configurations generated every 256 MCts. We note that for the adsorption energy $10kT$ and volume fraction $\Phi < 0.5$ considered in the simulations, the average lifetime of adsorbed chains is less than 1.2×10^5 MCts; i.e., each adsorbed chain experiences multiple desorption events during equilibration time and especially during the sampling time ($> 1.6 \times 10^7$MCts).

3. Results and Discussions

3.1. Bulk Properties of Head-to-Tail Associating Polymers. Before we discuss the results for the adsorbed polymer layers, we briefly recall the main properties of the head-to-tail associating polymers in the bulk. The chain length distribution for the reversibly associated linear chains in the bulk follows the exponential form:[12]

$$P(N) \propto \exp(-N/\langle N\rangle) \tag{1}$$

The average number or oligomers per chain, $\langle N\rangle$, noticeably increases with oligomer volume fraction Φ and energy of association $\Delta F/kT = \Delta E_{compl}/kT - \Delta S$ (where ΔS is the entropic loss associated with orientational specificity of reversible bonding[15]) as[12]

$$\langle N\rangle \sim \Phi^{1/2} \exp\frac{\Delta F}{2kT} = (\Phi K)^{1/2} \tag{2}$$

where K is the association constant: $K = \exp(\Delta F/kT)$.

The chain length distribution and the average number of oligomers per chain obtained in our simulations for associating polymers in the bulk (i.e., in the absence of adsorbing surface or far away from it) follow the expected dependence very well (see Supporting Information), similar to the previously reported simulation results.[12,16] We note that eqs 1 and 2 are valid for sufficiently long chains formed at large oligomer concentrations. At low concentrations, formation of rings (especially monomolecular) becomes important.[10,13,15] As we mentioned above, exclusive surface affinity for the donors eliminates the possibility of ring formation for adsorbed chains. At the same time rings from the bulk can still indirectly participate the end-adsorption process following ring-opening.

3.2. Density Profile for Adsorbed Chains. Typical monomer density profiles for the end-adsorbed polymers are shown in Figure 2 as a function of the distance to the surface for different bulk volume fractions of head-to-tail associating polymer, Φ. As is seen in all cases the density profile is essentially exponential, except for the immediate vicinity of the surface. (We note that a dip seen at the distance $z = 3a$ is an artifact of the BFM restricting the minimal distance between monomers.) For all densities of adsorption sites studied, the obtained density profile resembles neither the Gaussian-like profile expected for the mushroom regime of monodisperse end-grafted polymers[40−42] nor the parabolic density profile known for the brush regime.[36,43,44] The main reason for this is the large polydispersity of reversibly associated chains in the bulk[10,12] where the chain length distribution follows the exponential function $P(N) = (1$

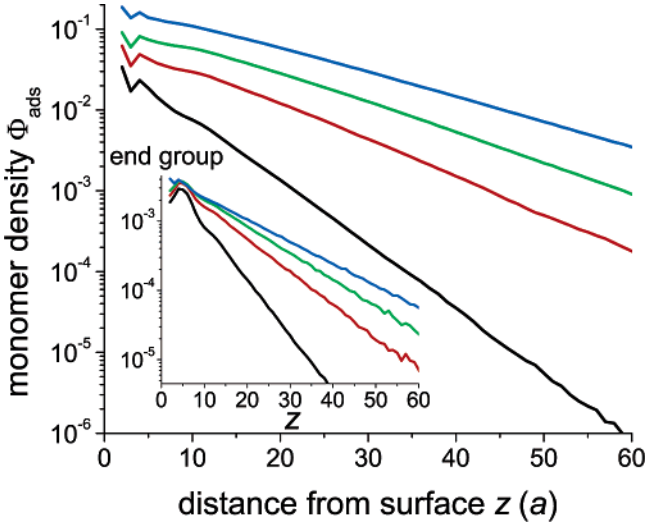

Figure 2. Monomer and end group (inset) density profiles for reversible polymer layer at an adsorbing site density $\sigma = 7.81 \times 10^{-3}a^{-2}$ and varying bulk polymer volume fraction $\Phi = 0.286$, 0.121, 5.56×10^{-2}, and 1.12×10^{-2} (from top to bottom).

$- q)q^N$ (with q being the probability of association for linear chains and N is the number of oligomers per chain).[10] As is discussed in the literature, the chain length distribution of living polymers retains its exponential form in the presence of surfaces[16] which is expected to translate into an exponential density profile for polymers end-adsorbed from dilute solutions on the surface with a low density of adsorption sites.[22,24] On the other hand, in the canonical simulations of living polymerization from a surface (where chain growth occurs via end-monomers) the density profile and the end group distribution obtained for a larger density of initial monomers were found to follow a power-law distribution with exponents of $-2/3$ and -2, respectively.[22] Our simulations show that the overall appearance of the density profile remains exponential for all densities of adsorption sites σ and polymer volume fractions in the bulk, Φ:

$$\Phi_{ads}(z) \sim \exp(-z/\xi). \tag{3}$$

Moreover, we found that the decay length ξ is independent of σ (any deviations are not systematic and well within a range of accuracy of our data), but it does depend on the (number) average chain length of the polymer in the bulk:

$$\xi \sim \sqrt{\langle N \rangle} \tag{4}$$

A similar chain length dependence was expected for dilute solutions and at low density of adsorption sites[24] based on assumption of Gaussian statistics: $\xi \sim R_g^{bulk} \sim \sqrt{\langle N \rangle}$. As is seen from Figure 3 the scaling dependence ($\xi \sim N^{1/2}$) holds rather well especially for longer chains end-adsorbed from bulk solution at higher polymer concentrations. We note that the dependence of the decay length on the average chain length (eq 4) remains valid also for reversibly associated polymers with a lower energy of complexation $\Delta E_{compl} = 8kT$ (and correspondingly lower adsorption energy $\Delta E_{ads} = \Delta E_{compl}$, shown as circles in Figure 3). The average chain length is somewhat shorter in this case compared to that at higher association energy for the same bulk polymer concentration. As we expect for eq 4 to hold also for different oligomer lengths, we added to Figure 3 two additional data points obtained for intermediate bulk concentrations of end-adsorbing head-to-tail associating oligo-

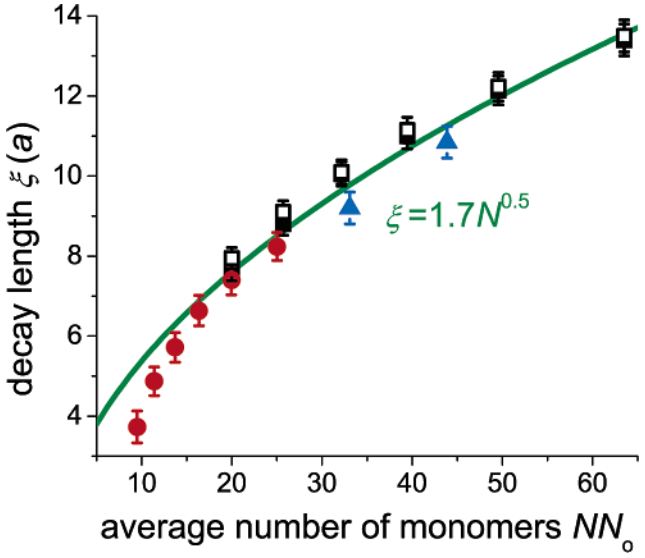

Figure 3. Decay length ξ corresponding to the density profile of reversibly associated layers (solid symbols) and distribution of free ends of adsorbed chains (open symbols) vs the average number of monomers in a polymer chain in the bulk. The squares are the results of simulation for $\Delta E_{assoc} = 10kT$ while the circles are obtained for $\Delta E_{assoc} = 8kT$ both using oligomer of length 4. The triangles are results for oligomer length $N_o = 8$ at $\Delta E_{assoc} = 10kT$.

mers of longer length $N_o = 8$ ($\Delta E_{compl} = 10kT$). As is seen, the data fit well to the same overall dependence.

Even though the interconnection between the average chain length and volume fraction of polymer in the bulk is relatively complicated,[10,15] in the limit of large association energies or concentrated solutions ($\Phi K \gg 1$) it follows a rather simple dependence, eq 2. As a result, the increase in ξ with an increase of $\langle N \rangle$ translates into the following scaling dependence

$$\xi \sim \Phi^{1/4} \text{ for } \Phi K \gg 1 \tag{5}$$

We have also studied the end group distribution for the adsorbed polymers (as shown in the inset of Figure 2), which also follows the exponential dependence with exactly the same decay length ξ as for the density profile. At a low density of adsorption sites and low bulk polymer volume fraction one can expect that the chains from the bulk will adsorb on the surface without significantly changing their length, so the probability to find a chain of N oligomers on the surface is the same as in the bulk. If this assumption is correct (as will be justified below), then one can obtain the end group density profile for adsorbed chains simply by superposition of the individual end group distributions: $\rho_{end}(z) = \int_0^\infty P(N)\rho_{end}(N, z)\, dN$ (where $\rho_{end}(N, z) = 2z(cN)^{-1}e^{-z^2/(cN)}$ is the end group distribution[45] for a single Gaussian chain of N oligomers and $c = 2N_o l^2/3$ with l being a bond length)

$$\rho_{end}(z) = \frac{4z(1-q)}{c} K_0\left(2z/\sqrt{\frac{c}{-\ln q}}\right) \tag{6}$$

with K_0 is the zeroth-order modified Bessel function of the second kind. Using the asymptotic form of K_0, we have

$$\rho_{end}(z) \approx \frac{2\sqrt{\pi z}(1-q)}{c}\left(\frac{c}{-\ln q}\right)^{1/4} e^{-2z/\sqrt{c/(-\ln q)}} \tag{7}$$

for large z. Since in the continuous limit ($q \to 1$), $-\ln q \approx 1 - q$ and $\langle N \rangle \approx (1 - q)^{-1}$,[10] the decay length becomes $\xi \approx \sqrt{c\langle N \rangle}/2 \approx l\sqrt{\langle N \rangle N_o/6} = A\sqrt{\langle N \rangle}a$ (with $A \approx 1.6-2.5$ for $N_o =$

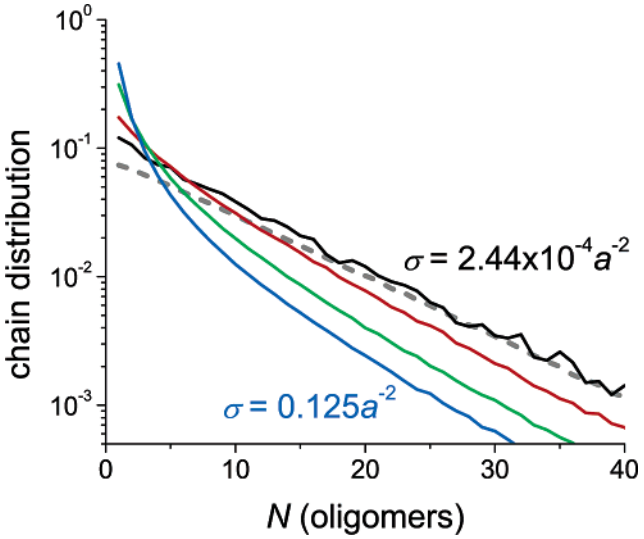

Figure 4. Chain length distribution for adsorbed chains at different adsorption site densities: $\sigma = 2.44 \times 10^{-4}a^{-2}$, $7.81 \times 10^{-3}a^{-2}$, $3.13 \times 10^{-2}a^{-2}$, and $0.125a^{-2}$ at the volume fraction $\Phi = 0.121$. Chain length distribution in the bulk for the same volume fraction is shown as the dashed line.

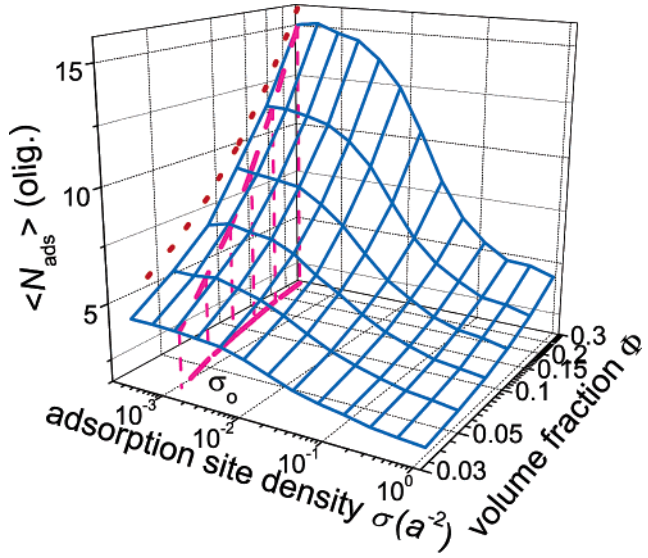

Figure 5. Average number of oligomers per adsorbed chain $\langle N_{ads}\rangle$ as a function of adsorption site density and polymer volume fraction. The dotted curve shows the $\langle N\rangle$ in the bulk while the dashed vertical wall corresponds to σ_o (when polymer chains on the surface start to overlap).

4 depending on the bond length in BFM) in agreement with eq 4. The results for the decay length ξ obtained from the end group density profiles are shown in Figure 3 (open symbols) for the same association energies and oligomer lengths as the monomer density profiles. As is seen, the decay length for both the monomer density profile and end group distribution is essentially the same and depends only on the length of head-to-tail associating chains in the bulk (and therefore the polymer volume fraction Φ), but not the density of adsorption sites σ.

3.3. Chain Length Distribution for Adsorbed Chains. Taking into account the exponential dependence of the monomer and end group density profiles, the chain length distribution in the adsorbed polymer layer must have some exponential form. In general for associating polymers it is known that longer chains are less likely to be found in a vicinity of a neutral surface.[16,18−20] On the other hand, for an adsorbing surface it was recently predicted that the chain length of adsorbed polymer will be larger than in the bulk.[21,46] Figure 4 shows the chain length distribution in the adsorbed polymer layer for an intermediate bulk volume fraction $\Phi = 0.121$ and different densities of adsorption sites. As expected, the distribution indeed has exponential form, at least for larger N values. Comparing the chain length distribution for head-to-tail associating polymers in the bulk and adsorbed on the surface, one can see that at a low density of adsorption sites σ these distributions are very similar (Figure 4). That ensured the success of our superposition approach at low Φ (eqs 6 and 7). At the same time, with increasing σ the chain length distribution changes: the probability to find short chains adsorbed on the surface noticeably increases, exceeding its value for the bulk, whereas longer chains become more rare. This trend becomes stronger as the density of adsorption sites increases. At the same time the tail of the distribution maintains its exponential form with a very similar slope (on the semilog scale of Figure 4) as for the bulk chain length distribution. This similarity of the exponential decay for chain length distributions in the adsorbed layer and in the bulk is the origin for eq 5 which relates the decay length for the density profile of adsorbed polymers to the average volume fraction of polymer in the bulk. The tails of the longer chains adsorbed on the surface are surrounded by the bulk polymer and as a result behave in a very similar manner, resulting in the exponential dependence for both the density profile and chain length distribution. Indirect evidence of the exponential chain length dependence in the end-adsorbed polymer layer is provided by recent AFM measurements[7] where an exponential chain length dependence was observed for the probability of stretching a supramolecular chain that bridges the gap between the substrate and tip.

Figure 5 shows the change in the average number of oligomers per adsorbed chain, $\langle N_{ads}\rangle$ as a function of both the polymer volume fraction in the bulk (Φ) and the density of adsorption sites on the surface, σ. As is seen at low σ, $\langle N_{ads}\rangle$ for adsorbed polymer is rather similar to that in the bulk, $\langle N\rangle$ (dotted curve) especially at larger Φ. For small, Φ the (number) average chain length of adsorbed polymers is somewhat smaller than that in the bulk, but since chains are rather short at that concentration this difference is not so noticeable on the scale of the plot. With an increase in the density of adsorption sites σ, the chain length distribution shifts toward shorter chains and as a result the average number of oligomers per adsorbed polymer chain decreases. The decrease in the average chain length becomes especially noticeable when adsorbed chains start to overlap on the surface. This occurs when the average distance between adsorbed chains becomes comparable to twice the average end-to-end distance for adsorbed chains $\langle R_e\rangle$ ($\langle R_e\rangle_{bulk}$ for bulk polymers can serve as an estimate since chain overlap on the surface starts at very low σ). The corresponding density of adsorption sites σ_o is shown in Figure 5 as a dashed vertical wall. As is seen σ_o indicates rather well the point at which $\langle N_{ads}\rangle$ starts to decline. This decrease is especially noticeable for higher polymer concentrations Φ, for which the average chain length is longer. (Experimentally the average chain length of end-adsorbed supramolecular polymers was also found to be smaller than in the bulk.[7−9]) Since the (number) average length of adsorbed polymer increases with an increase of polymer volume fraction Φ and decreases with an increase in the density of adsorption sites σ, the longest chains adsorbed on the surface are observed at large Φ and low σ. We note that the weight-average chain length qualitatively follows the same behavior as the number-average chain length, except the decrease in the former is less pronounced and becomes noticeable at a larger density of adsorption sites. As a result, the polydispersity of

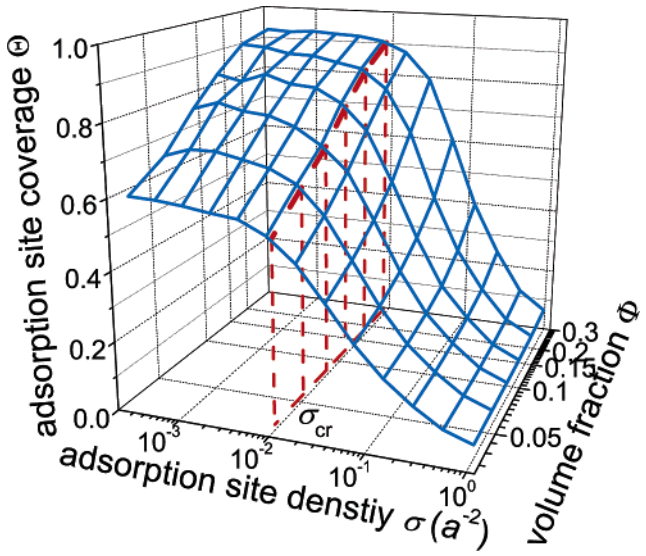

Figure 6. Fraction of occupied adsorption sites as a function of the adsorption site density and bulk volume fraction of polymer. The vertical dashed wall corresponds to σ_{cr} (when oligomers adsorbed on the surface start to overlap).

adsorbed polymer chains is in the range of 1.5−2 (depending on polymer concentration for bulk solutions), increasing to 1.5−3.5 at larger σ. The increase in polydispersity observed for more concentrated solutions is attributed to the increase in the population of short chains, which leads to considerable decrease in the number-average molecular weight, while weight-average molecular weight is less affected by it. For dilute solutions the average chain length is rather small, so that both number and weight-average values are equally affected and polydispersity practically does not change.

3.4. Surface Coverage. Another important property of the adsorption process is surface coverage, which in our case corresponds to the fraction of occupied sites, Θ. We plot in Figure 6 the fraction of occupied sites as a function of adsorption site density σ and bulk polymer volume fraction Φ. As is seen for a given Φ, Θ remains nearly constant until some critical density of adsorption sites σ_{cr} above which it decreases rapidly. Comparing the fraction of occupied sites Θ for different volume fractions of bulk polymer one can notice that the decrease in the surface coverage starts practically at the same critical density of adsorption sites σ_{cr}. Being independent of volume fraction of polymer in the bulk, σ_{cr} cannot depend on average chain length or correlation length, both of which are functions of concentration. Since the smallest polymer which can adsorb on the surface is simply an oligomer, σ_{cr} must be related to the oligomer length, the unique parameter for the system considered. Indeed, comparing half of the average distance between the adsorption sites ($0.5\sigma^{-1/2}$) with the end-to-end distance of oligomers attached to the surface R_e^{olig}, one finds that when the two become equal to each other, the oligomers start to overlap. Using MC simulations we have calculated the probability of neighboring adsorbed oligomers to overlap p_o as a function of the distance between the neighbors. Plotting p_o and the fraction of occupied sites Θ on the same graph (Figure 7) vs the minimal distance between the adsorption sites one can observe that the former starts to increase at the same time as the latter starts to decrease. We have repeated our simulations for a longer oligomer chain length $N_o = 8$ and compared again p_o and Θ for this oligomer length. In this case, the amount of adsorbed polymer is somewhat less than for the shorter oligomer length and a decrease in Θ starts at larger average distance

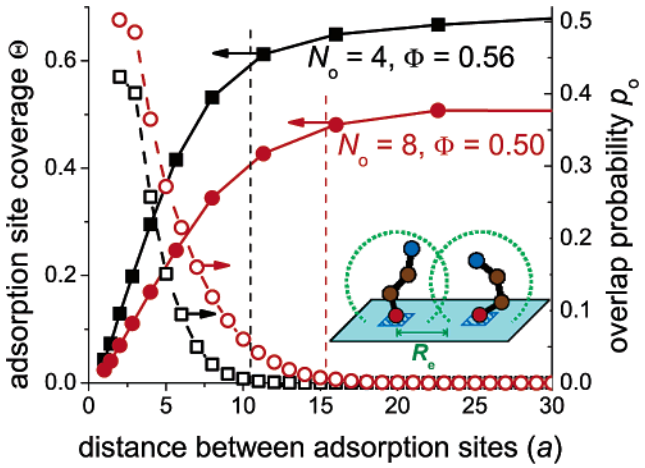

Figure 7. Fraction of occupied adsorption sites (filled symbols and solid lines) and the overlap probability for neighboring oligomers on the surface (open symbols and dashed lines) as functions of the minimal distance between adsorption sites. The vertical dashed lines mark the distances at which neighboring oligomers start to overlap.

between the adsorption sites. As is seen from Figure 7, for both oligomer lengths $N_o = 4$ and $N_o = 8$, the decrease in the fraction of occupied sites starts at the σ_{cr} corresponding to the overlap distance for the respective oligomer length. Encouraged by this observation we can expect that this pattern of behavior may be valid for longer oligomer lengths as well. It remains to be seen experimentally whether this prediction will hold, but on the basis of our simulation results, we expect that for head-to-tail associating polymers the surface coverage remains constant until some critical density of adsorption sites

$$\sigma_{cr} \simeq (2R_e^{olig})^{-2} \tag{8}$$

above which neighboring oligomers start to overlap.

As is seen from Figure 6, a larger fraction of occupied sites is achieved at higher volume fraction of polymer for all σ considered. On one hand, this result is not surprising, as for end-adsorbing monodisperse polymers or diblock copolymers, it is known that the surface coverage increases with an increase in polymer concentration in the bulk.[26,28,30] On the other hand the surface coverage is known to decrease with an increase of molecular weight of end-adsorbing chemically bonded polymers.[26,28,30,31] For reversibly associated polymers the average chain length increases with polymer volume fraction (eq 2), so that one could expect smaller surface coverage for longer chains if one extrapolates the results for chemically bonded polymers. Obviously this is not the case. The increase of bulk concentration (i.e., providing more chains to adsorb) evidently has a stronger effect on the adsorption process compared to the increase of chain length which makes it harder for chains to reach the surface due to the conformational penalties. The important difference is that head-to-tail associating polymers can "adsorb in stages". First, a single oligomer can come to the surface and adsorb, then another one can associate with the adsorbed one and so on. Thus, accessibility of the surface is not an issue for the reversibly associated polymers as long as the oligomer length is small enough.

3.5. Average Height. To characterize the average thickness of adsorbed reversibly associated polymer layer we have calculated the average height $\langle h \rangle$ based on the density profile:

$$\langle h \rangle \equiv \int_0^\infty z\Phi_{ads}(z)\, dz \tag{9}$$

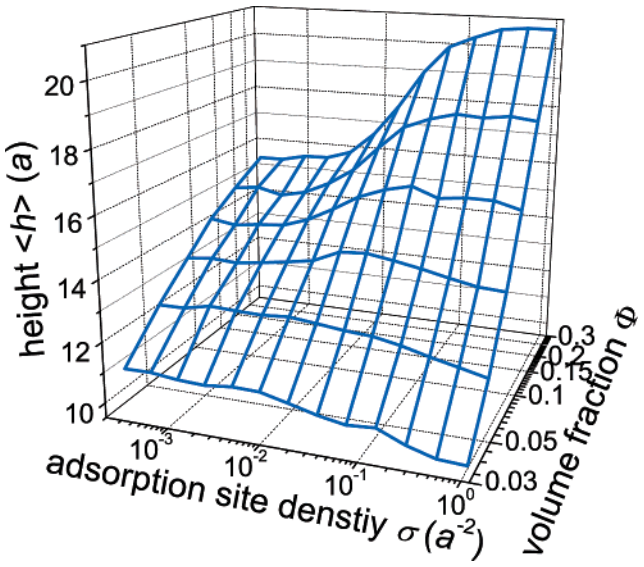

Figure 8. Average height of the adsorbed polymer layer as a function of adsorption site density and bulk polymer volume fraction.

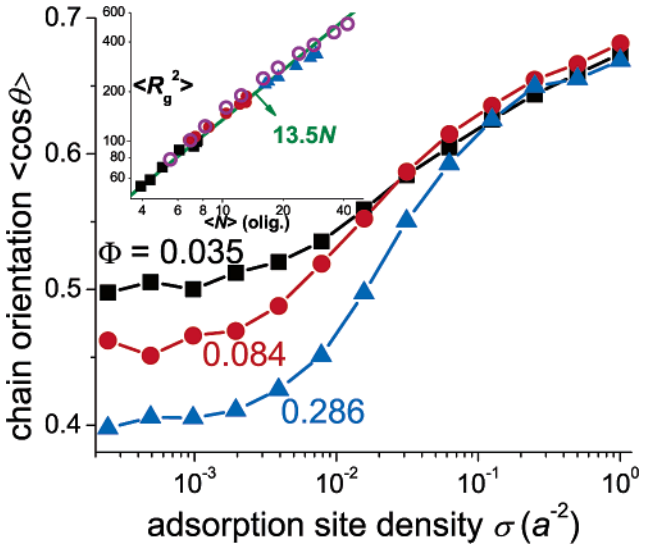

Figure 9. Average orientation $\langle\cos\theta\rangle$ of long principal axis of R_g of adsorbed polymer with respect to the surface normal as a function of adsorption site density for different bulk polymer volume fractions. The dependence of the average square radius of gyration, $\langle R_g^2\rangle$ vs average number of oligomers in adsorbed chains at different densities of adsorption sites (symbols are the same as in the main plot) is shown in the inset in comparison with the results for bulk chains (open circles).

The average height of the adsorbed polymer layer is shown in Figure 8 as a function of density of adsorption sites σ and polymer volume fraction in the bulk Φ. As expected, the largest height of adsorbed layer is achieved at a higher bulk volume fraction of polymer. With an increase of σ, the average height starts to increase for the layers adsorbed from more concentrated bulk polymer solutions (large Φ) and it stays the same or slightly decreases for dilute bulk solution (small Φ). We note that in the case of end-grafted chemically bonded polymers the height of polymer layer increases with an increase of grafting density due to the mushroom to brush conformational transformation,[43,47] when neighboring chains start to overlap on the surface; i.e., it would occur as early as σ_o (see Figure 5), if we dealt with end-grafted polymers of constant length. In our case the amount of adsorbed polymers and their length self-adjust, so that σ_o signifies the point when the adsorbed chains starts to overlap on the surface and their chain lengths start to decline to avoid chain stretching. As a result, nothing noticeable happens to the height of the layer at that point. At a somewhat higher density of adsorption sites (σ_{cr}), neighboring oligomers start to overlap leading to the decrease in the fraction of occupied sites Θ. Again, nothing significant happens with the height of the brush at that point as well.

To determine whether the mushroom-to-brush conformational transformation occurs for associated end-adsorbed polymers, we analyzed the average radius of gyration $\langle R_g\rangle$ for adsorbed polymers as a function of an average number of oligomers per chain $\langle N_{ads}\rangle$. We found that the overall dependence remains practically the same as in the bulk. As is seen from the inset of Figure 9, the average square radius of gyration $\langle R_g^2\rangle$ scales as $\langle N_{ads}\rangle^x$ with $x = 1-1.1$ as one can expect for concentrated to dilute solutions of polymers with excluded volume (ensured by BFM rules). Since the data obtained for adsorbed polymers follow a very similar dependence as that in the bulk $\langle R_g^2\rangle_{bulk}$, we conclude that end-adsorbed polymers on the surface are not stretched on average. This result is not totally surprising as for end-adsorbed polymers polymer brush regime can be achieved only at high adsorption energies[25,28] otherwise chains are only slightly extended compared to the bulk.[31] For head-to-tail reversibly associated polymers, the chain lengths of adsorbed polymer decrease with an increase in the density of adsorption sites, so that polymer does not become stretched. At the same time, the average height of the adsorbed polymer layer increases for large volume fractions of polymer in the bulk as is seen in Figure 8. We found that the enhancement in chain orientation (in the direction perpendicular to the surface) is responsible for the increase of the height.

To characterize the chain orientation we have calculated principal moments of inertia for adsorbed chains and analyzed the angle θ between the surface normal and the long axis R_g^l of the ellipsoid formed by a chain. As is seen from Figure 9, at low σ polymers adsorbed from dilute solution do not have any preferable orientation (except for the small volume exclusion effect enforced by the surface) and the average value of cos θ is about 0.5. With an increase in σ chains adsorbed from dilute solution start to feel the presence of neighbors and as a result orient more in the direction perpendicular to the surface with $\langle\cos\theta\rangle \simeq 0.67$. For polymer chains adsorbed from more concentrated solutions at a low density of adsorption sites, the chains orient more along the surface ($\langle\cos\theta\rangle \approx 0.4$). This is due to the fact that the depletion zone near the surface for larger bulk polymer concentration is more narrow,[21] so that the adsorbed polymers tend to orient along the surface where the local polymer concentration is lower than in the bulk. Another factor which may also contribute to chain alignment along the surface is the presence of orientationally specific (and therefore more rigid) donor−acceptor bonds, which tend to orient along the surface in its close vicinity. With an increase in the density of adsorption sites, σ, polymer chains adsorbed from more concentrated solutions start to overlap at lower σ as their average length is longer and as a result their orientation starts to change leading to an increase in $\langle\cos\theta\rangle$. This increase occurs more abruptly compared to that for chains adsorbed from dilute solutions; however, the final values of $\langle\cos\theta\rangle \approx 0.67$ reached at larger σ are comparable (Figure 9).

Thus, the height of the adsorbed polymer layer depends on at least two factors: the radius of gyration of adsorbed chains (related to chain length) and chain orientation. In particular, the product of the average cos θ and the average long axis R_g^l

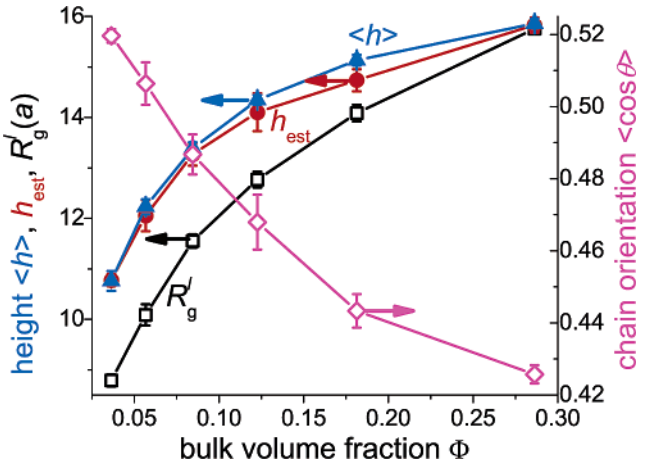

Figure 10. Average height of the adsorbed polymer layer (triangles) at the adsorption site density $\sigma = 3.9 \times 10^{-3}a^{-2}$ as a function of bulk polymer volume fraction in comparison with $h_{est} = 2.36\ \langle R_g^l \rangle \langle \cos\theta \rangle$ (circles). The long axis component of the radius of gyration $\langle R_g^l \rangle$ is shown as open squares, whereas $\langle \cos\theta \rangle$ characterizing the chain orientation with respect to the surface normal is shown as open diamonds (right axis).

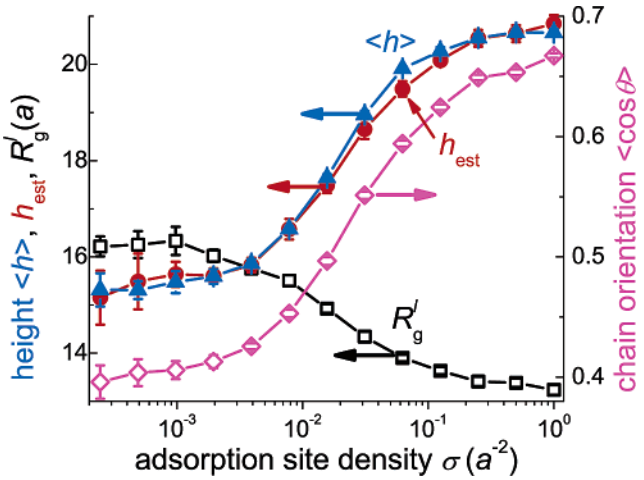

Figure 11. Average height of the adsorbed polymer layer (triangles) at the polymer bulk volume fraction $\Phi = 0.286$ as a function of adsorption site density in comparison with $h_{est} = 2.36\ \langle R_g^l \rangle \langle \cos\theta \rangle$ (circles). The long axis component of the radius of gyration $\langle R_g^l \rangle$ is shown as open squares, whereas $\langle \cos\theta \rangle$ characterizing the chain orientation with respect to the surface normal is shown as open diamonds (right axis).

of the ellipsoid formed by a chain can provide an estimate of an average height of the adsorbed layer:

$$\langle h \rangle \approx 2.36 \langle R_g^l \rangle \langle \cos\theta \rangle \tag{10}$$

We note that the empirical numerical factor 2.36 which provides the best match between the approximation (eq 10) and the simulation data for the height of the layer, is between $\sqrt{6}$ corresponding to the end-to-end distance ($R_e^2 = 6R_g^2$) and $\sqrt{5}$ related to the radius of a sphere of a constant density with the second moment equal to R_g^2.

First we consider the change in the height of the adsorbed polymer layer as a function of concentration at constant density of adsorption sites. We chose $\sigma = 3.9 \times 10^{-3}(a^{-2})$ to be just below σ_{cr}. As is seen from Figure 10, with an increase in Φ the radius of gyration increases following the chain length ($\langle R_g \rangle \sim \langle N \rangle^{1/2}$). On the other hand, shorter polymer chains adsorbed at low polymer concentration are somewhat more oriented perpendicular to the surface ($\langle \cos\theta \rangle \approx 0.53$) compared to the long chains adsorbed from concentrated bulk solution ($\langle \cos\theta \rangle \approx 0.43$). As we mentioned above, the main reason for this effect is the decrease of the depletion zone with an increase of polymer concentration forcing chains to stay closer to the surface. This orientation effect does not overcome the increase in the radius of gyration with an increase of Φ, so that the product of the two (eq 10) increases as well (Figure 10). We note that eq 10 provides a very good estimate for the height of the adsorbed layer.

The change in the height of the adsorbed polymer layer with an increase in density of adsorption sites is considered in Figure 11 for high polymer concentration. At low σ the chain orientation and (the long axis of) the radius of gyration remains nearly unchanged. A further increase in σ is accompanied by the noticeable decrease in R_g^l resulting from continuous chain shortening caused by the overlap of neighboring chains on the surface. At the same time, an increase in the number of adsorbed chains leads to the enhancement of chain orientation perpendicular to the surface. At larger polymer volume fractions the increase in $\langle \cos\theta \rangle$ is especially noticeable as chains change their orientation from being slightly aligned along the surface ($\langle \cos\theta \rangle \approx 0.43$) at low σ to being more oriented perpendicular to the surface ($\langle \cos\theta \rangle \approx 0.67$) at a large density of adsorption sites. As a result, the increase in orientation dominates the decrease in the chain radius of gyration and the height of the polymer layer increases (Figure 11). Analyzing the distribution of cos θ as a function of the number of repeat units in the chain, N, we conclude that the increase in the average cos θ values is primarily due to the orientation of short chains located next to the surface (see Supporting Information). The orientation of long chains remains essentially unaffected by the increase of σ beyond the level of isotropic orientation. A very similar behavior was observed for living polymerization from the surface studied by Milchev et al.[22] They found that chain segments located near the surface are preferably oriented perpendicular to the surface, while segments located more far away along the chain have no preferred orientation.

The increase of the height of the end-adsorbed reversibly associated polymers with an increase in the surface density was also observed experimentally in recent AFM measurements.[9] The height of the adsorbed layer indicated some degree of stretching, although it could be attributed to electrostatic interactions and the larger intrinsic rigidity of the chains, which would enhance orientational effects compared to the case considered here.

At lower polymer concentrations the height of the adsorbed polymer layer does not change appreciably or may slightly decrease with σ (Figure 8). In this case, an increase in chain orientation with an increase in σ is less pronounced since even at low σ chains are already excluded from the surface. As a result, the decrease in chain length with an increase in σ may overcome the orientational effect leading to the slight decrease in the average height of adsorbed layers. We note these two counteracting trends are very close in magnitude leading to larger uncertainty range in prediction of the average height for low polymer concentrations (see Supporting Information).

3.6. Diagram of States for End-Adsorbed Reversibly Associated Chains. In Figure 12, we summarize the different regimes of behavior for reversibly associated polymers end-adsorbed on surfaces. It is worthwhile to note that none of the boundaries in the state diagram (Figure 12) represent phase transitions: all measured properties of the system vary continuously from one regime to another. At a low volume fraction of

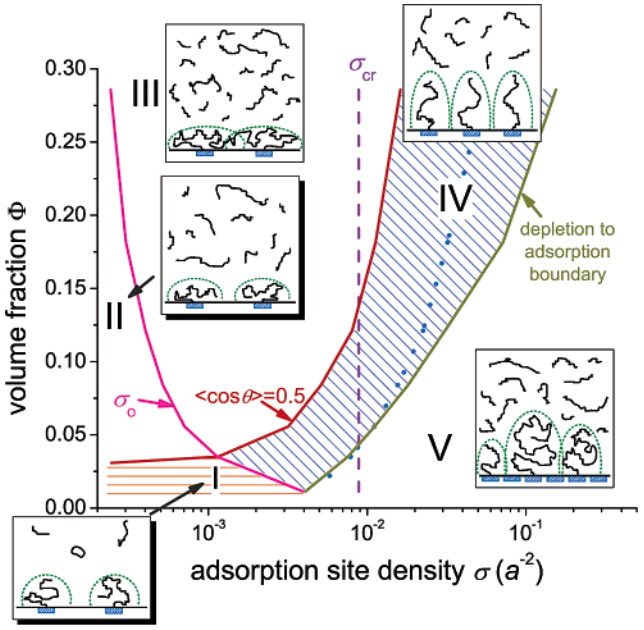

Figure 12. Diagram of states for end-adsorbing reversible polymer layer showing the following regimes: normal mushroom (I), compressed mushroom (II), overlapping compressed chain (III), overlapping elongated chain (IV), and overlapping dissociating chain (V). The vertical dashed line is $\sigma = \sigma_{cr}$. The dotted curve corresponds to the case when the density profile of adsorbed chains can be reproduced by superposition of individual chain profiles (obtained in zero-concentration limit).

polymer in the bulk and a low density of adsorption sites the adsorbed polymer chains form a *normal mushroom* regime (I); i.e., individual chains adsorbed on the surface do not feel their neighbors, and their conformation (and chain length distribution) is rather similar to that in the bulk except for surface-induced volume exclusion. The height of the polymer layer is defined by the average radius of gyration, as expected. At a low density of adsorption sites an increase in the volume fraction of polymer in the bulk results in formation of a *compressed mushroom* regime of adsorbed chains (II), when adsorbed chains do not influence each other, but their orientation is influenced by the bulk polymer: the higher is the Φ, the smaller is the average value of cos θ (between the long axis of ellipsoid formed by the chain and the *z*-direction perpendicular to the surface); i.e., chains are more spread along the surface than extended away from it. As we discussed above, this behavior is related to the decrease of the depletion zone near the surface with an increase in Φ. The boundary between the *normal mushroom* (I) and *compressed mushroom* (II) regimes is defined by the condition $\langle\cos\theta\rangle = 0.5$ which corresponds to the average value of cos θ for isotropically oriented chains. The values of $\langle\cos\theta\rangle < 0.5$ correspond to "compressed chains" oriented more along the surface than perpendicular to it. The height of the polymer layer increases with bulk polymer concentration.

With an increase in the density of adsorption sites chains adsorbed on the surface start to overlap at $\sigma_o(\Phi)$ (see Figure 5), which serves as an upper boundary of the *compressed mushroom* (II) regime. As we discussed above, the overlap limit for chains adsorbed at higher bulk concentrations is reached at lower σ since the chain length is larger in this case. At $\sigma > \sigma_o$, density of chains near the surface increases, while the length of adsorbed chains start to decrease (compared to that in the bulk) to avoid stretching. Among adsorbed chains, short ones become oriented more perpendicular to the surface, while longer chains, which dominate the distribution, are still in the "compressed state" i.e., $\langle\cos\theta\rangle < 0.5$, so the overall adsorbed layer is in *the overlapping compressed chain* (III) regime. The height of the polymer layer in this regime starts to increase compared to the mushroom regime height. Further increasing σ brings us to the limit when neighboring oligomers adsorbed on the surface start to overlap ($\sigma = \sigma_{cr}$) (see eq 8 and Figure 6). Beyond this point, the fraction of occupied adsorbed sites starts to decrease with an increase in σ since some of the adsorption sites are blocked by the neighboring adsorbed chains. At a density of adsorption sites slightly larger than σ_{cr} for high bulk polymer volume fractions or slightly smaller than σ_{cr} for a lower Φ, the chain orientation reaches an isotropic level; i.e., $\langle\cos\theta\rangle = 0.5$. This is the boundary between the *overlapping compressed chain* (III) and *overlapping elongated chain* (IV) regime. In regime IV, the density of polymer in the adsorbed layer reaches a sufficiently high level so that at some density of adsorption sites σ (shown as a dotted curve in Figure 12) the chain conformation becomes similar to that of freely standing chains in the zero concentration limit. At that point, the density profile of adsorbed chains can be reproduced by superposition of individual chain profiles as described in subsection 3.2. As σ increases chains become more oriented in the direction perpendicular to the surface. The strong orientation enhancement dominates over the decrease in the average chain length (radius of gyration) leading to the noticeable increase in the height of the polymer layer with an increase in σ as we discussed in the previous section (Figure 11). The increase in the height of the layer is the most pronounced at high bulk polymer volume fraction where the chain length of adsorbed (and bulk) polymers is the largest and the impact of the orientational rearrangement is the strongest. We note that even through the local concentration of polymer in the immediate vicinity of the surface can exceed the average bulk concentration, the total concentration of the polymer (both adsorbed and free) within the polymer layer remains less than in the bulk. At the low volume fraction of polymer in the bulk the region IV is bounded by the overlap density, σ_o limiting region I of the *normal mushroom*.

Further increase in the density of adsorption sites σ diminishes the depletion tendency and at some point, which serves as a boundary between *overlapping elongated chain* (IV) (or *normal mushroom* regime I) and *overlapping dissociating chains* (V), adsorption starts to prevail. In region V, the average concentration of the polymer (both adsorbed and free) within the polymer layer becomes comparable or exceeds that in the bulk. Because of the reversible nature of chain association further increase of polymer density near the surface triggers oligomer redistribution from the adsorbed to bulk polymers. As a result, the chain length of adsorbed polymers continues to decrease while further enhancement of orientation of the chains perpendicular to the surface direction is limited to short chains only. Thus, in this regime, chain shortening becomes the dominant factor, ultimately leading to the leveling off or even the decrease of adsorbed layer height.

In our current simulations we have considered a specific case of adsorption energy being the same as association energy $\Delta E_{compl} = \Delta E_{ads}$. This will be the case if either donor or acceptor groups similar to that of the bulk polymer are deposited on the surface. If the adsorption energy ΔE_{ads} is different compared to ΔE_{compl}, then the adsorption behavior can be somewhat altered compared to the diagram of states discussed above. For instance, if the adsorption energy is considerably smaller than the association energy ($\Delta E_{ads} \ll \Delta E_{compl}$) when one can expect a rather low surface coverage, with the adsorbed chain length being similar to that in the bulk. So one can expect to observe

regimes I, II, and possibly III in this case. In the opposite limit of very high adsorption energy ($\Delta E_{ads} \gg \Delta E_{compl}$) interaction with the surface is very favorable and as a result nearly all adsorption sites will be occupied. One can expect to see formation of a "monolayer" of one oligomer height on top of which adsorption of other oligomers will occur (with energy ΔE_{compl}) in a manner similar to what discussed in this paper. In general, a decrease of the adsorption energy will shift the diagram of states to the right; i.e., it will take larger density of adsorption sites to reach regimes III−V while the increase of the adsorption energy will shift it to the left: i.e., smaller σ will be needed to achieve regimes III−V due to higher average occupancy of the sites. Especially in the latter case appearance of other adsorption regimes may be possible as, e.g., mentioned above "monolayer" formation.

4. Conclusions

In this paper, we have applied Monte Carlo simulations to study reversible end-adsorption of head-to-tail associated polymers from the bulk. As the adsorption sites on the surface were attractive to donor groups only, no loop formation was possible on the surface. We have studied the effects of polymer volume fraction in the bulk Φ (for dilute to semidilute/concentrated solutions) and surface density of adsorption sites σ on the adsorption process and structure of the adsorbed polymer layer.

We found that the monomer and end group density of an adsorbed polymer layer follow an exponential dependence $\Phi(z) \sim \exp(-z/\xi)$ (at least at larger distances from the surface) for all studied bulk polymer concentrations and densities of adsorption sites. This form of the density profile is a reflection of the exponential chain length distribution in the bulk. The decay length ξ is found to be dependent mainly on the average chain length of polymer in the bulk and hence the polymer concentration: $\xi \sim N^{1/2} \sim \Phi^{1/4}$. Thus, the polymer layers adsorbed from more concentrated solution produce more slowly decaying density profiles compared to dilute solutions. The effect of the adsorption site density on the adsorbed monomer density profile mainly manifests itself in the increase of polymer density on the surface, without changing the shape of the profile. These results agree with the prediction by Besseling et al.[24] concerning the exponential dependence of the adsorbed monomer density for the case of dilute solutions of Gaussian chains in the low adsorption density limit.

The chain length distribution in the adsorbed polymer layer is found to follow an exponential dependence similar to the bulk, except for the enhancement of the contribution of short chain in the distribution. This enhancement becomes especially noticeable at a larger density of adsorption sites on the surface and low Φ. As a result, the average chain length in the adsorbed polymer layer is comparable with that in the bulk only at the lowest σ studied. As σ increases, the average chain length of adsorbed polymers decreases. This decrease becomes especially pronounced when chains on the surface start to overlap, i.e., $\sigma > \sigma_o$. Shortening the chain length diminishes the stretching of polymers inside the dense polymer layer formed on the surface. Experimentally, the average chain length of end-adsorbed supramolecular polymers was also found to be smaller than that in the bulk.[7−9]

With an increase in the density of adsorption sites, the fraction of occupied sites Θ (i.e., surface coverage) remains nearly constant up to some point (which is found to be independent of polymer concentration in the bulk), σ_{cr}, above which oligomers absorbed on the surface start to overlap. As a consequence, at $\sigma > \sigma_{cr}$ some fraction of adsorption sites get blocked, and Θ starts to decline. The surface coverage achieved by longer polymer chains (i.e., adsorbed from a more concentrated solution) always exceeds that for shorter chains (adsorbed from more dilute solutions), in contrast to what is known for chemically bonded polymers.[26,28,30,31] The main difference here is that chain length of head-to-tail associated polymers is related to the polymer volume fraction. Also, reversibly associated polymers are capable of "adsorbing in stages", i.e., by one oligomer at a time, which increases the accessibility of the surface.

The height of adsorbed polymer layer increases with an increase in the bulk polymer concentration. At a low density of adsorption sites, the height is related to the average radius of gyration for adsorbed chains, as expected for the mushroom regime. With an increase in σ the average height of the polymer layer adsorbed from concentrated solutions (large Φ) increases, while for polymer layers adsorbed from more dilute solutions the height remains practically at the same level as in the mushroom regime or even slightly decreases. These different patterns of the adsorbed chain behavior are summarized in the diagram of states (Figure 12), which can be applied for systems with different adsorption energies or spacer length than considered here. Analyzing the average radius of gyration of the adsorbed polymers $\langle R_g \rangle$ we found that polymer chains are not stretched: $\langle R_g \rangle \simeq \langle R_g^{bulk} \rangle$. This is the result of the reversible nature of the polymers: in order to reduce stretching the chain length of adsorbed polymers becomes shorter and the surface coverage remains at a moderate level. Nevertheless, the height of the adsorbed layer obtained for larger Φ increases with increasing σ. We found that the main reason for this is chain orientation perpendicular to the surface. At low σ, chains adsorbed from relatively concentrated solutions are preferably oriented along the surface (due to the narrow depletion zone). With an increase in σ, chains become more crowded on the surface and start to orient away from it. The larger is σ, the stronger is the chain orientation along the surface normal and hence the larger is the height of the layer. The increase of the height of the end-adsorbed reversibly associated polymers with an increase in the surface density was also observed experimentally in recent AFM measurements.[9]

Acknowledgment. This material is based upon work supported by the National Science Foundation under Grant No. 0348302.

Supporting Information Available: Figures showing bulk properties including chain length distribution for reversible associated polymers, average number of oligomers per chain as a function of oligomer number, average height of the adsorbed polymer layer, and average orientation $\langle \cos \theta \rangle$ of the adsorbed polymer long axis with respect to the surface normal. This material is available free of charge via the Internet at http://pubs.acs.org.

References and Notes

(1) (a) Lehn, J.-M. *Supramolecular Chemistry: Concepts and Perspectives*; VCH: Weinheim, Germany, 1995. (b) Lehn, J.-M. *Science* **2002**, *295*, 2400−2403.
(2) Prins, L. J.; Reinhoudt, D. N.; Timmerman, P. *Angew. Chem., Int. Ed.* **2001**, *40*, 2382−2426.
(3) ten Cate, A. T.; Sijbesma, R. P. *Macromol. Rapid Commun.* **2002**, *23*, 1094−1112.
(4) Zou, S.; Schönherr, H.; Vancso, G. J. *J. Am. Chem. Soc.* **2005**, *127*, 11230−11231.
(5) Xu, J.; Craig, S. L. *J. Am. Chem. Soc.* **2005**, *127*, 13227−13231.
(6) Kersey, F. R.; Yount, W. C.; Craig, S. L. *J. Am. Chem. Soc.* **2006**, *128*, 3886−3887.

(7) Zou, S.; Schönherr, H.; Vancso, G. J. *Angew. Chem., Int. Ed.* **2005**, *44*, 956−959.
(8) Kersey, F. R.; Lee, G.; Marszalek, P.; Craig, S. L. *J. Am. Chem. Soc.* **2004**, *126*, 3038−3039.
(9) Kim, J.; Liu, Y.; Ahn, S. J.; Zauscher, S.; Karty, J. M.; Yamanaka, Y.; Craig, S. L. *Adv. Mater.* **2005**, *17*, 1749−1753.
(10) Jacobson, H.; Stockmayer, W. H. *J. Chem. Phys.* **1950**, *18*, 1600−1606.
(11) Flory, P. J. *Principles of Polymer Chemistry*; Cornell University Press: Ithaca, NY, 1953.
(12) (a) Cates, M. E.; Candau, S. J. *J. Phys.: Condens. Matter* **1990**, *2*, 6869−6892. (b) Wittmer, J. P.; Milchev, A.; Cates, M. E. *J. Chem. Phys.* **1998**, *109*, 834−845.
(13) Milchev, A.; Wittmer, J. P.; Landau, D. P. *Phys. Rev. E* **2000**, *61*, 2959−2966.
(14) Dudowicz, J.; Freed, K. F.; Douglas, J. F. *J. Chem. Phys.* **1999**, *111*, 7116−7130.
(15) (a) Chen, C.-C.; Dormidontova, E. E. *Macromolecules* **2004**, *37*, 3905−3917. (b) Chen, C.-C.; Dormidontova, E. E. *J. Am. Chem. Soc.* **2004**, *126*, 14972−14978.
(16) Milchev, A.; Landau, D. P. *J. Chem. Phys.* **1996**, *104*, 9161−9168.
(17) Rouault, Y.; Milchev, A. *Macromol. Theory Simul.* **1997**, *6*, 1177−1190.
(18) Schmitt, V.; Lequeux, F.; Marques, C. M. *J. Phys. II Fr.* **1993**, *3*, 891−902.
(19) van der Gucht, J.; Besseling, N. A. M. *Phys. Rev. E* **2002**, *65*, 051801.
(20) Feng, E. H.; Fredrickson, G. H. *Macromolecules* **2006**, *39*, 2364−2372.
(21) van der Gucht, J.; Besseling, N. A. M.; Fleer, G. J. *Macromolecules* **2004**, *37*, 3026−3036.
(22) Milchev, A.; Wittmer, J. P.; Landau, D. P. *J. Chem. Phys.* **2000**, *112*, 1606−1615.
(23) van der Gucht, J.; Besseling, N. A. M.; Stuart, M. A. C. *J. Am. Chem. Soc.* **2002**, *124*, 6202−6205.
(24) van der Gucht, J.; Besseling, N. A. M.; Fleer, G. J. *J. Chem. Phys.* **2003**, *119*, 8175−8188.
(25) Marques, C. M.; Joanny, J. F. *Macromolecules* **1989**, *22*, 1454−1458.
(26) Ligoure, C.; Leibler, L. *J. Phys. (Paris)* **1990**, *51*, 1313−1328.
(27) Milner, S. T. *Macromolecules* **1992**, *25*, 5487−5494.
(28) Lai, P.-Y. *J. Chem. Phys.* **1993**, *98*, 669−673.
(29) Clancy, T. C.; Webber, S. E. *Macromolecules* **1993**, *26*, 628−636.
(30) (a) Zhan, Y.; Mattice, W. L.; Napper, D. H. *J. Chem. Phys.* **1993**, *98*, 7502−7507. (b) Zhan, Y.; Mattice, W. L.; Napper, D. H. *J. Chem. Phys.* **1993**, *98*, 7508−7514.
(31) Zajac, R.; Chakrabarti, A. *Phys. Rev. E* **1994**, *49*, 3069−3078.
(32) Kopf, A.; Baschnagel, J.; Wittmer, J.; Binder, K. *Macromolecules* **1996**, *29*, 1433−1441.
(33) Rodgers, S. D.; Santore, M. M. *Macromolecules* **1996**, *29*, 3579−3582.
(34) Titmuss, S.; Briscoe, W. H.; Dunlop, I. E.; Sakellariou, G.; Hadjichristidis, N.; Klein, J. *J. Chem. Phys.* **2004**, *121*, 11408−11419.
(35) Field, J. B.; Toprakcioglu, C.; Dai, L.; Hadziioannou, G.; Smith, G.; Hamilton, W. *J. Phys. II* **1992**, *2*, 2221−2235.
(36) Fleer, G. J., Cohen Stuart, M. A., Scheutjens, J. M. H. M., Cosgrove, T., Vincent, B., Eds.; *Polymers at interfaces*; Chapman and Hall: London, 1993.
(37) Wittmer, J. P.; Cates, M. E.; Johner, A.; Turner, M. S. *Europhys. Lett.* **1996**, *33*, 397−402.
(38) (a) Carmesin, I.; Kremer, K. *Macromolecules* **1988**, *21*, 2819−2823. (b) Deutsch, H. P.; Binder, K. *J. Chem. Phys.* **1991**, *94*, 2294−2304.
(39) Metropolis, N.; Rosenbluth, A.; Rosenbluth, M.; Teller, A.; Teller, E. *J. Chem. Phys.* **1953**, *21*, 1087−1092.
(40) Hesselink, F. T. *J. Phys. Chem.* **1969**, *73*, 3488−3490.
(41) Dolan, A. K.; Edwards, S. F. *Proc. R. Soc. London A* **1974**, *337*, 509−516.
(42) de Gennes, P. G. *Macromolecules* **1980**, *13*, 1069−1075.
(43) (a) Milner, S. T.; Witten, T. A.; Cates, M. E. *Macromolecules* **1988**, *21*, 2610−2619. (b) Milner, S. T. *Science* **1991**, *251*, 905−914.
(44) (a) Skvortsov, A. M.; Pavlushkov, I. V.; Gorbunov, A. A.; Zhulina, Y. B.; Borisov, O. V.; Pryamitsyn, V. A. *Polym. Sci. USSR* **1988**, *30*, 1706−1715. (b) Zhulina, E. B.; Borisov, O. V.; Priamitsyn, V. A. *J. Colloid Interface Sci.* **1990**, *137*, 495−511.
(45) (a) Tanaka, T. *Macromolecules* **1977**, *10*, 51−54. (b) Douglas, J. F.; Nemirovsky, A. M.; Freed, K. F. *Macromolecules* **1986**, *19*, 2041−2054.
(46) Zweistra, H. J. A.; Besseling, N. A. M. *Phys. Rev. Lett.* **2006**, *96*, 078301.
(47) Evers, O. A.; Scheutjens, J. M. H. M.; Fleer, G. J. *J. Chem. Soc., Faraday Trans.* **1990**, *86*, 1333−1340.

MA061236B